Image particle sizing of an air blasted liquid sheet of kerosene at intermediate pressure

C. Hennig[1*], F. Giuliani[1], S. Freitag[2], C. Hassa[2]
[1]Institute for Thermal Turbomachinery and Machine Dynamics,
Graz University of Technology, Graz, Austria
[2]Institute of Propulsion Technology,
DLR e.V. - German Aerospace Center, Cologne, Germany

Abstract

This paper presents a method of image processing to analyze the atomization of a prefilming airblast atomizer. The results of this analysis are based on atomization images obtained by previous experiments performed with kerosene on a flat liquid sheet airblast atomizer at intermediate pressure and room temperature (Bhayaraju [1]). The main objective of this study is to investigate the successive atomization process and to evaluate a correlation for droplet size distributions which can be used to specify the spray in numerical simulations [2] and to understand the atomization regimes for an appropriate introduction of the liquid phase. In the prefilming atomizer the closed tube-shaped original film is modeled as a flat film for both optical access and ease of manipulation. The 2-D laboratory atomizer had a prefilmer length of 4 mm and an injection slit of 0,3 mm. The evaluated images show the prefilmer surface and the primary breakup zone and are analyzed by classifying the size and position of ligaments and droplets. Due to various changes in liquid mass flow, air pressure and air velocity it is possible to obtain size distributions for a wide range of parameters. All analysis was done using a self-developed image processing code based on Matlab. In this paper, we focus on the width and length of the attached ligaments. Based on these shape parameters probability density functions are estimated for the intermediate status of atomization at the prefilmer lip.
This study is based on a collaboration of DLR Cologne and TU Graz and is supported by the Austrian Science Fund (FWF).

Introduction

Airblast atomization has set the standard for liquid fueled gas turbines. It provides a refined atomization at low energy cost, which combined to a swirl-stabilized flame leads towards high power and low pollutant emissions [3]. One major task in research is to get a better understanding of the atomization process. In the process of primary atomization a stream of liquid interacts with faster airstreams causing the liquid to break up into ligaments. Secondary atomization means the further breakup into finer droplets. Atomization can be described with help of the Weber number, which is the dimensionless ratio of momentum force to surface force [4].

$$We = \frac{\rho_{air} v_{air}^2 t_{liq}}{\sigma_{liq}} \tag{1}$$

However, rising pressure and air velocity makes the successive breakup mechanisms harder to differentiate. We propose here a systematic analysis of non-spherical particle sizes in the direct vicinity of the injector lip as a function of different operating conditions. So Marmottant and Villermaux [5] analyzed the breakup of a round liquid jet while Bharayaju [1] investigated the liquid sheet breakup of a flat prefilming airblast atomizer under pressure with no vaporization.

Digital imaging of the atomization process is of great importance for advanced knowledge on its characteristics. Based on digital imaging particle size measurements can performed [7]. So the ambition of this study is to apply image analyzing techniques on Bharayaju's images showing the zone of primary breakup of injected kerosine and receive a correlation to his Phase Doppler Anemometry (PDA) measurements done in the far field. This will lead to a better understanding and knowledge of the primary atomization process which could help in modeling two-phase flows.

* Corresponding author, christoph.hennig@tugraz.at

Experimental Setup

This study is based on experiments done by Bhayaraju [1] on the fuel spray test rig at German Aerospace Center Cologne. The tests were done in the LPP test rig where atomization processes can be observed under realistic conditions. This facility was originally conceived for a lean premixing and prevaporisation (LPP) burner study.

The test section is depicted in Figure 1: it consists of an inner glass channel made of Herasil for high temperature measurements, surrounded by a peripheral cooling duct. A set of 3 high-pressure windows provide optical access. The volume of investigation is *40 x 40 x 200 mm*. A 2-D prefilming airblast atomiser with transparent 4 mm prefilming surface was used to model the closed tube-shaped original film as a flat film for both optical access and ease of manipulation. The operating conditions with importance on this study are given in Table 1. All Experiments were done under room temperature. PDA measurements were done in the far field (*90 mm* axial distance to atomizer) with a constant liquid film load of *366 g/s/m* which correspondents to a liquid mass flow rate of $q_{liq} \approx 4\ g/s$.

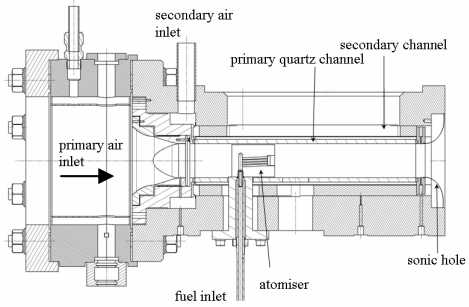

Figure 1. Experimental test section (top view)

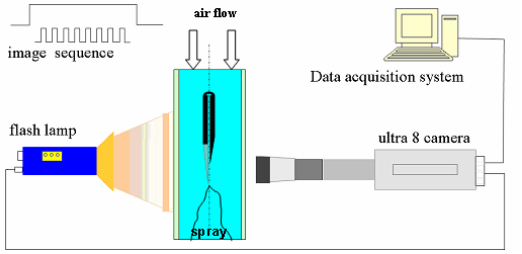

Figure 2. Background lightning setup (side view)

Table 1. Operating Conditions

p_{air} [bar]	2	2	2	2	3	3	3	3	6	6	6	6	6	6	6	6
v_{air} [m/s]	30	30	60	60	30	30	30	30	30	30	60	60	60	60	60	60
q_{liq} [g/s]	4	6	4	6	2	4	6	7,5	4	6	3	4	5	6	7	8
We	31	30	129	127	48	47	45	44	92	89	384	381	378	375	372	369

Instrumentation and data processing

To obtain a view on breakup mechanisms background lightning was adopted. The Ultra 8 high-speed camera from DRS Hadland ltd is used to capture the images, illuminated by a Bowens 1500 flash lamp. The imaging area is *8 x 8 mm* picturing the prefilmer's lip and its successive flow (Figure 2). We refer on images seen from the top, with the hypothesis of a thin depth-of-field limiting sizing errors. Because of the integration effect of side views, the following process cannot directly used.

For the quantitative analysis performed on the resulting spray, PDA measurements were conducted focusing on the spatial distribution of liquid fuel flux and *SMD* at the maximal possible axial distance of *90 mm* to the atomizer. A Dantec 2-D PDA system was used to measure the axial and the vertical droplet velocities and the droplet diameters. Further information can be found in [1].

Image Processing

In order to obtain any valuable information from the images, it is necessary to perform some operations on the data before ligament analysis can start. The first task is a binarization of all images which is then followed by the identification and marking of the ligaments using a floodfill algorithm.

Due to the background lightning the liquid is represented by different shades of gray in the images. To identify ligaments it is essential to have information on what is liquid and what is air. Binarization can provide such information since it transforms a graylevel image into a binary image with the information *1* (liquid) and *0* (air). The simplest way to binarize an image is to set one threshold and compare every single pixel value to it. If the pixel value is below the threshold this value is set to zero otherwise it is set to one. The difficulty lies in setting the right threshold.

Since there are image parts displaying liquid by having a different brightness one global threshold would be deficient. In our case one dataset consists of 100 images for each parameter variation. Based on this 100 images the threshold matrix T is calculated :

$$T(x_i, y_i) = \frac{\sum_{i=1}^{n} I(x_i, y_i)}{n} \tag{2}$$

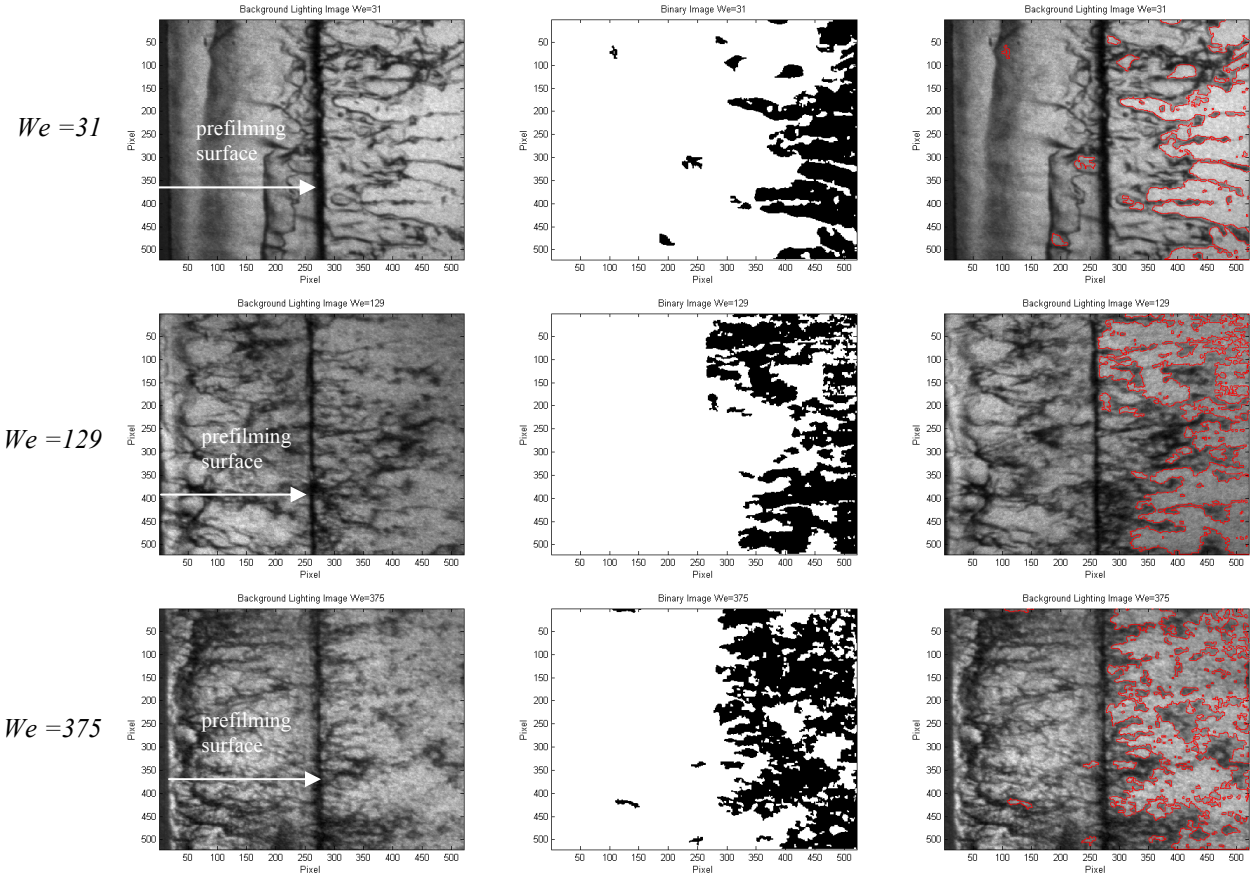

Figure 3. Image Binarization with different *We*

original image	binarized image	contour of ligaments
low intensity: liquid	white: liquid	low intensity: liquid
high intensity: air	black: air	high intensity: air

Figure 3 shows the result of the binarization method applied to a dataset where an early liquid sheet break-up is observed. Dark patterns in the grayscale image representing liquid are mapped by white patterns in the binary image. Applying this binarization method on images where liquid sheet break-up can be seen at the end of the prefilmer's lip leads to unsufficient results. Images of those datasets show larger ligaments with less contrast to the air flow. Hence another approach must be used. Instead of using a threshold matrix based on all images of a series a so called adaptive threshold as proposed by Niblack [6] is used. This implies one single threshold matrix for each particular image. The threshold matrix T is computed with the mean value m and the standard deviation s around the coordinates x,y with the constant $k = 0.9$:

$$T(x, y) = m(x, y) - k \cdot s(x, y) \tag{3}$$

As mentioned before, ligaments are identified via a floodfill algorithm. This algorithm is commonly used by paint programs to fill regions with defined borders with one color. After binarization the ligaments are represented

by single white regions. To identify particular ligaments the recursive scanline floodfill algorithm is applied on each binary image. During this operation the images are searched for pixels with the value *1*. Once such a pixel is found its connected pixels are identified both iteratively and recursively and the identified ligament is marked by a marker represented by a unique color (Figure 4).

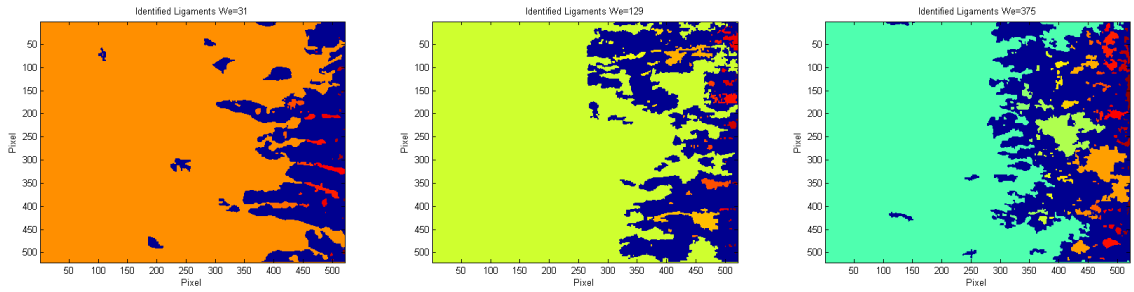

Figure 4. Ligament identification. Each ligament is marked with an individual color.

Once the identification process is done, an analysis of the ligaments is done by measuring their height, width and area. It is possible to gain information on the surface waves propagating on the prefilming surface. To make a comparison between the image processing technique and the PDA measurements an equivalent *SMD* is calculated based on the area information of the ligaments. For this *SMD* a ligament diameter is estimated based on a spherical droplet with the same 2-D sectional area as the ligament .

$$D_{eq} = 2\sqrt{\frac{A_{lig}}{\pi}} \tag{4}$$

$$SMD_{eq} = \frac{\sum N_i D_{eq}^3}{\sum N_i D_{eq}^2} \tag{5}$$

Results and Discussion

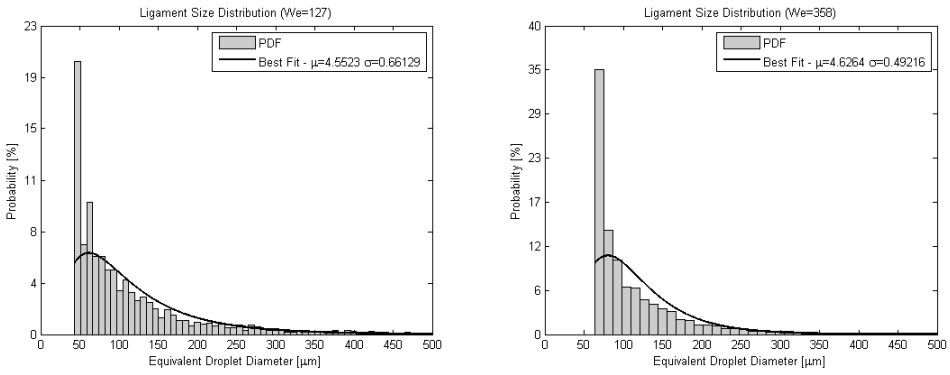

Figure 5. PDF of D_{eq} at different *We* with log-normal fit (primary atomization)

The probability distribution functions for D_{eq} as shown in Figure 5 are evaluated for the different Weber numbers. These functions were fitted with several distribution functions. The best fitting distribution in matter of the determination coefficient is the log-normal distribution with the parameters μ and σ:

$$f(D_{eq}) = \frac{1}{D_{eq}\sigma\sqrt{2\pi}} e^{\frac{-(\ln(D_{eq})-\mu)^2}{2\sigma^2}} \tag{6}$$

The parameter μ gives the equivalent droplet size with the highest counting while σ presents the shape parameter. An evaluation of these fitted log-normal distributions shows the dependency of the parameters on the Weber number. While μ decreases with increasing *We*, the shape parameter stays rather constant at $\sigma \approx 0.7$. There is a wider spreading for both parameters at low *We* (Figure 6 left and middle). The rapidly decrease of μ at *We>400* can be explained by surface stripping as it was found by Bharayaju for a prefilming atomiser. At low Weber numbers a thin liquid sheet is formed over the prefilming surface. An increase of the Weber number (i.e. increase of v_{air} to v_{liq} ratio, increase of p_{air}) leads at first to the propagation of surface waves and finally the shearing-off of the liquid sheet. So at higher Weber numbers the momentum exchange between the liquid and air increases and smaller ligaments are formed which leads to a finer atomisation in the far field. Hence the *SMD* decreases at increasing *We*.

A closer examination of the surface waves in axial direction is depicted in Figure 6 (right). The plot shows the wavelength λ as a function of p_{air} with the parameter q_{liq} at v_{air}=*30 m/s*. For the higher liquid mass flow rate longer surface waves are propagated. For both liquid mass flow rates λ follows a similar power law as a function of p_{air}. At higher v_{air} surface stripping gets dominant and wavelengths could not be determined from the images. The wider spreading of the parameters at low *We* can also be explained by the effect of surface stripping. The liquid sheet covers the whole prefilming surface at low *We* and breaks up into large ligaments at the surface's end. An increase in *We* causes surface stripping and an early breakup into numerous small ligaments which leads to more regular size distributions.

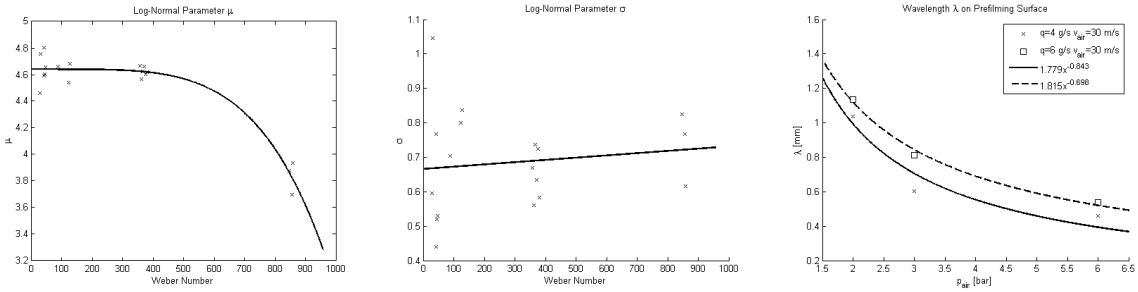

Figure 6.
left and middle: Log-Normal parameters as a function of *We*
right: Wavelength of surface waves

A comparison of Image Processing and PDA measurement is shown in Figure 7 with the *SMD* as a function of *We*. As mentioned before the PDA measurements done by Bhayaraju were performed with a constant liquid velocity of 1 m/s. To compare both methods the images used for the right plot were those taken under the same liquid flow parameters. Both results show a power law dependence of the *SMD* from the *We* with the same exponential decrease and a variation by the factor *6.1*.

Since the equivalent *SMD* is derived from images showing the top view of the primary breakup zone no information on the thickness of the ligaments is given. The results of the equivalent *SMD* are implying a linear correlation between ligament sizes and PDA measurements. Since the physics of atomization also strongly depends on liquid mass flow more data from the far field at different liquid mass flow rates is needed for validation.

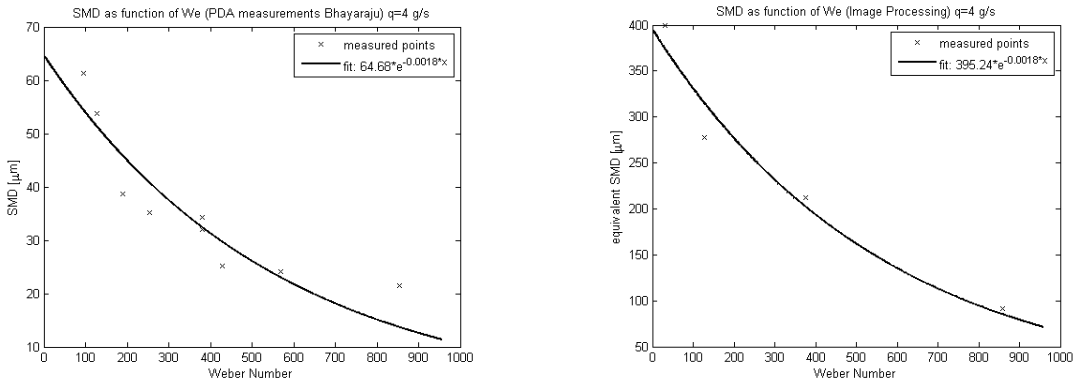

Figure 7. SMD as a function of Weber number
left: PDA measurements (far field) - right: image processing (primary breakup zone, attached ligaments)

Conclusions

An operational set of tools for analyzing liquid sheet breakup into ligaments in the vicinity of the injector has been developed and tested on images of a flat airblasted liquid sheet. As a result ligament sizes were correlated with size distributions obtained by PDA measurements done in the far field. A future use of the image analyzing technique on pulsed atomization is planned.

Nomenclature

T	threshold matrix
I	graylevel intensity
n	quantity of images per dataset
N	number of ligaments
x,y	coordinates
m	mean of x,y-environment intensities
s	standard deviation of x,y-environment intensities
k	constant
q	mass flow rate
ρ	density
p	pressure
v	velocity
t	thickness
σ_{liq}	liquid surface tension
We	Weber number
μ,σ	parameter of log-normal distribution
SMD	Sauter Mean Diameter
D	diameter

Subscripts

air	air
liq	liquid
eq	equivalent size
i	index

References

1. U. Bhayaraju, *Liquid Sheet Breakup and Characterusation of Plane Prefilming and Nonprefilming Atomisers,* DLR-Forschungsbericht 2008-02, 2008
2. P. Trontin1,S. Vincent, J. Estivalezes, J. Caltagirone, *Detailed comparisons of front-capturing methods for turbulent two-phase flow simulations,* Int. J. Numer. Meth. Fluids 56:1543–1549(2008)
3. A.H. Lefebvre, *Atomization and Sprays*, Hemisphere Publishing Corporation, 1989
4. R. Clift, J.R. Grace, M.E. Weber, *Bubbles, Drops, and Particle,* Academic Press, 1978
5. P. Marmorttant and E. Villermaux, *On spray formation,* J. Fluid Mech. 498:73-111(2004)
6. W. Niblack, *An Introduction to Digital Image Processing*, Prentice-Hall, 1986
7. H. Malot, J. Blaisot, *Droplet Size Distribution and Spericity Measurements of Low-Density Sprays Through Image Analysis*, Part. Part. Syst. Charact 17:146-158 (2000).

Acknowledgments

The research activities were supported by the Austrian Science Fund (FWF, project: P 20530-N13) which is gratefully acknowledged. U. Bharayaju is also acknowledged.